Available online at www.sciencedirect.com
ScienceDirect
Journal of Volcanology and Geothermal Research 156 (2006) 291–301
Journal of volcanology and geothermal research
www.elsevier.com/locate/jvolgeores

Using trace element correlation patterns to decipher a sanidine crystal growth chronology: An example from Taapaca volcano, Central Andes

Georg F. Zellmer [a,b,*], Jorge E. Clavero [c]

[a] *Institute of Earth Sciences, Academia Sinica, 128 Academia Road, Section 2, Nankang, Taipei 11529, Taiwan, ROC*
[b] *Lamont-Doherty Earth Observatory, 61 Route 9W, Palisades, New York 10964, USA*
[c] *Servicio Nacional de Geología y Minería, Av. Santa María, 0104-Santiago, Chile*

Received 23 December 2004; accepted 2 March 2006
Available online 2 May 2006

Abstract

Sanidine megacrysts occur in a number of dacite lava domes of young volcanic edifices in the Central Andes of Northern Chile. Trace element variations within a sanidine crystal erupted in a 14.1 ± 1.4 ka old dacite lava dome from Taapaca volcano are studied here to decipher its crystal growth chronology using trace element diffusion systematics. The trace element concentration profiles were determined by ion microprobe at 80 μm stepwidth across a total core to rim profile length of ~2.5 cm. The crystal displays large variations in Sr and Ba content, with wavelengths of trace element variations down to <160 μm. Clear growth zone boundaries outbound of the distinct crystal core are absent at this sampling density. Strong correlation of Sr with Ca and the virtual lack of correlation of Ba with Ca are shown to be consistent with intracrystalline diffusion of Sr subsequent to crystal growth. Despite the complicated crystal growth history, correlation analysis across the crystal yields 4 diffusion ages of individual growth segments at a magmatic temperature of 875 °C, ranging from ~1300 years close to the core to ~550 years at the crystal rim, implying an effective crystal growth rate of $\sim 1.2 \times 10^{-10}$ cm s^{-1}. The short residence time at high temperature indicates that the magma from which the crystal grew was stored in a small and ephemeral upper crustal reservoir, and was likely remobilized just prior to its eruption by intrusion of hot, more mafic magma, as suggested by the abundance of mafic enclaves within the dacite lava dome.

Keywords: diffusion; geospeedometry; sanidine; arc magmatism; remobilization

1. Introduction

In a number of studies the crystal record has been used to constrain both open and closed system magmatic processes (e.g., Anderson, 1983, 1984; Pearce and Kolisnik, 1990; Stamatelopoulou-Seymour et al., 1990; Blundy and Shimizu, 1991; Singer et al., 1993; Davidson and Tepley, 1997; Knesel et al., 1999; Anderson et al., 2000; Davidson et al., 2000). These contributions have been successful in constraining magmatic processes such as crystallization, convection, crystal fractionation and retention, magma recharge and mixing, and crustal assimilation. However, it has rarely been possible to constrain the rates of these processes

* Corresponding author. Institute of Earth Sciences, Academia Sinica, 128 Academia Road, Section 2, Nankang, Taipei 11529, Taiwan, ROC. Tel.: +886 2 2783 9910x602; fax: +886 2 2783 9871.
E-mail address: gzellmer@earth.sinica.edu.tw (G.F. Zellmer).

0377-0273/$ - see front matter © 2006 Elsevier B.V. All rights reserved.
doi:10.1016/j.jvolgeores.2006.03.004

and the timing of specific magmatic events that are necessary to fully understand the dynamics of the magmatic system at depth. It would be of great advantage if the chemical record could be linked to a chronological record of crystal growth.

There are a number of techniques available to constrain crystallization timescales, including crystal size distribution studies (e.g., Cashman and Marsh, 1988; Marsh, 1988; Higgins, 1996a, b, 2000), and mineral isochron dating using the Rb–Sr system (e.g., Christensen and DePaolo, 1993; Davies and Halliday, 1998), U–Th isotopes (e.g., Taddeucci et al., 1967; Allègre, 1968; Allègre and Condomines, 1976; Pyle et al., 1988; Condomines, 1997; Reid et al., 1997; Heath et al., 1998; Zellmer et al., 2000) and Ra–Th isotopes (e.g., Volpe and Hammond, 1991; Volpe, 1992; Cooper et al., 2001; Turner et al., 2003). Mineral isochron studies are based on the assumption of rapid crystallization, which may in some cases be violated (Charlier and Zellmer, 2000; Turner et al., 2003). Alternatively, if the temperature of the magma is known, the residence times of individual crystals may be determined by modelling the diffusive equilibration of elements within and between crystals (e.g., Gerlach and Grove, 1982; Humler and Whitechurch, 1988; Kohn et al., 1989; Nakamura, 1995; Morgan et al., 2004). Sr and Mg diffusion within plagioclase crystals has recently led to the determination of residence times of this major mineral phase (Zellmer et al., 1999; Costa et al., 2003; Zellmer et al., 2003).

Alkali feldspar megacrysts have been documented in many volcanic settings (e.g., Chapman and Powell, 1976; Bahat, 1979; Guo et al., 1992) and their large size offers the opportunity to date consecutive crystal growth zones and the potential to combine relative and absolute dating techniques, such as Sr-diffusion and U–Th isotope ages. In this contribution, we study the growth chronology of a large sanidine crystal from a dacite lava dome of Taapaca volcano in the Central Andes of Northern Chile (cf. Fig. 1), and show that relative dating techniques can be used despite the complicated growth history of this crystal.

2. Geological background

The Taapaca volcanic complex (TVC), also known as Nevados de Putre, is part of the Andean Central Volcanic Zone, Northern Chile, and is located on the western margin of the Altiplano at 18°06′S, 69°30′W. The geology and stratigraphy of TVC are summarized in Fig. 2. According to previous work (Clavero, 2002; Clavero et al., 2004a,b, and references therein), Taapaca has evolved from a gently-dipping stratovolcano, formed by silicic andesite (60–61 wt.% SiO_2) lava flows in its first stage, to a voluminous steep-sided stratovolcano, formed by mainly dacitic (62–68 wt.% SiO_2) lavas, domes and their associated block-and-ash flow and lahar deposits in its second stage. Finally, it evolved to become a dome complex during stages III and IV, mainly formed by dacitic (62–68 wt.% SiO_2) domes and their associated debris avalanches, blasts, tephra fallout, block-and-ash flow and lahar deposits, with most of the activity focused towards the southern and south-western flanks of the complex, where the main populated area of the Chilean Altiplano is located.

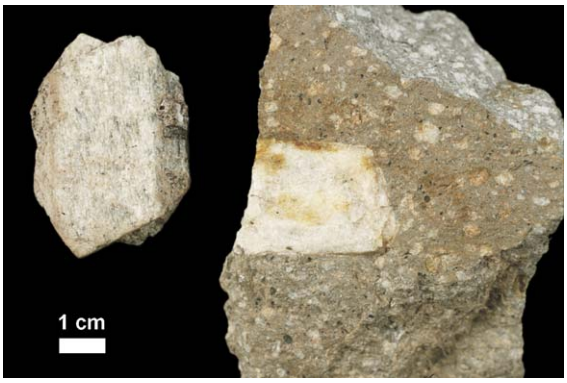

Fig. 1. Examples of twinned sanidine megacryst samples erupted in dacite lava domes from Taapaca volcano.

There are good geochronological constraints on the eruptive history of the volcano, with $^{39}Ar/^{40}Ar$ and radiocarbon dates from volcanic deposits ranging in age from ca. 1.5 Ma to 2.3 ka (Clavero, 2002; Clavero et al., 2004a,b). Late Pleistocene to Holocene activity (Stage IV) occurred in four discrete effusive-explosive phases, which have been cyclic during the last 100 ka, with each episode of dome growth and collapse lasting less than 10 ka (Clavero et al., 2004a,b). These intensive eruptive phases have been followed by relatively long quiescent periods (tens of thousands of years), during which no evidence of eruptive activity has been found. Volcanic activity has produced several sector collapses and their associated volcanic debris avalanches, and several dome explosions and collapses and their related blasts and block-and-ash flow deposits. The $^{39}Ar/^{40}Ar$ work includes ages of 38.2±3.1 and 14.1±1.4 ka (Clavero et al., 2004a,b; Clavero and Sparks, 2005) for the eruption of two sanidine megacrysts bearing dacite domes. The crystal studied in this contribution is taken from the latter dome.

Finally, Taapaca lavas show an increasing content of mafic enclaves through time, from none at Stage I to 5–

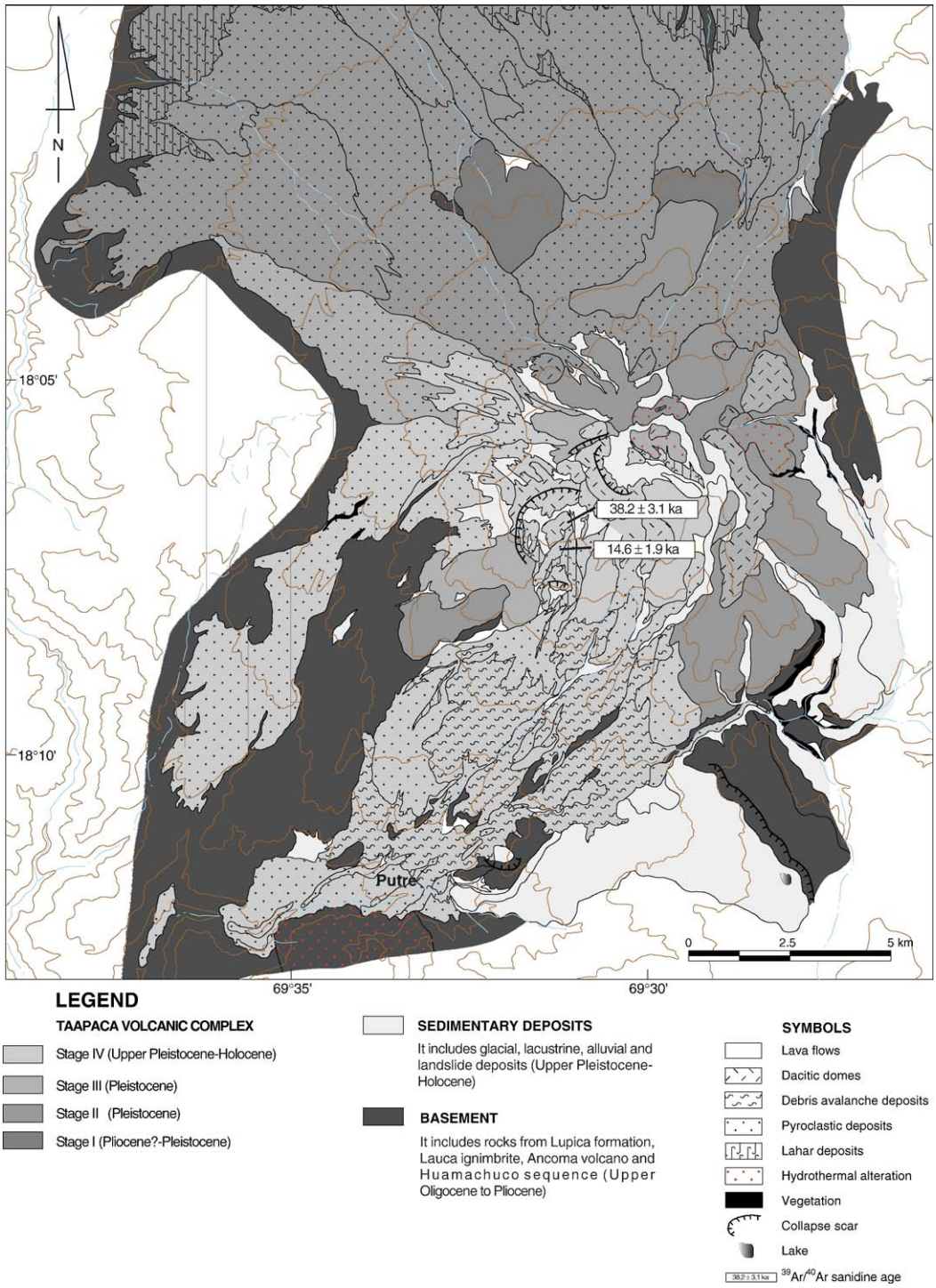

Fig. 2. Simplified geological map of the Taapaca Volcanic Complex, adapted from Clavero and Sparks (2005).

6% by volume in Stage IV deposits, suggesting that magma-mixing processes have become increasingly important in the later stages of volcanic evolution. Ubiquitous evidence of pre-eruptive magma mixing processes found in the deposits suggests that most of the eruptions have been triggered by the intrusion of new batches of hot andesitic magma into cooler, mainly dacitic reservoirs (Clavero, 2002).

3. Analytical techniques

Ion microprobe measurements were made on gold-coated polished probe sections of a 14.1 ± 1.4 ka old sanidine crystal using the Cameca ims-4f at Edinburgh University. A $^{16}O^-$ primary beam of 15 keV net energy and 5 to 9 nA beam current was used to sputter pits of ~15 μm diameter, in 80 μm steps from core to rim (Fig. 3). Sampling density was sufficiently detailed to characterize zoning wavelengths of up to 1 cm previously described for crystals from the 38.2 ka old dacite dome (Lohnert, 1999; Woerner et al., 2004). Positive secondary ions were accelerated through 4.5 keV into a double focusing mass spectrometer. Molecular ions were suppressed by use of energy filtering techniques (Zinner and Crozaz, 1986), using a 40 V energy bandpass to which a 75 V offset voltage was applied. Intensities for each element were measured on the electron multiplier at a single isotope in order of increasing mass, for between 2 and 8 s per peak over ten cycles. Element concentrations were calibrated using a combination of feldspar (SHF-1, Hill-32, Lake County) and borosilicate glass standards, at variable step widths. Their ion yields had patterns similar to NBS SRM 610 (Hinton, 1990), but their overall ionisation efficiency relative to Si was 15% to 30% lower. This is consistent with previous measurements of these reference samples. Absolute element concentrations are accurate to better than 10% (1σ), but relative variations in concentration across a single crystal could be resolved to better than 2% (1σ).

4. Results

In the absence of electron probe data, the relative (ionization efficiency corrected) ion probe count rates of K, Na and Ca, were used to calculate the proportions of orthoclase, albite and anorthite. X_{Or} is given in Fig. 4a, and displays small variations around 0.65, with a drop to more sodic sanidine towards the crystal rim. The data were filtered for plagioclase inclusions with extremely low X_{Or} content. Sanidine stoichiometry was then used to obtain absolute values of SiO_2 from the relative proportions of feldspar endmember compositions. Absolute concentrations of trace element concentrations, of which Sr and Ba are given as core to rim profiles in Fig. 3b and c, were then calculated from their count rates relative to Si. Analyses contaminated by microinclusions of oxides were excluded based on extremely high Ti and Mg contents. Trace element variations are relatively small within the crystal core (0–5040 μm), around 1100 ppm for Sr and ranging from

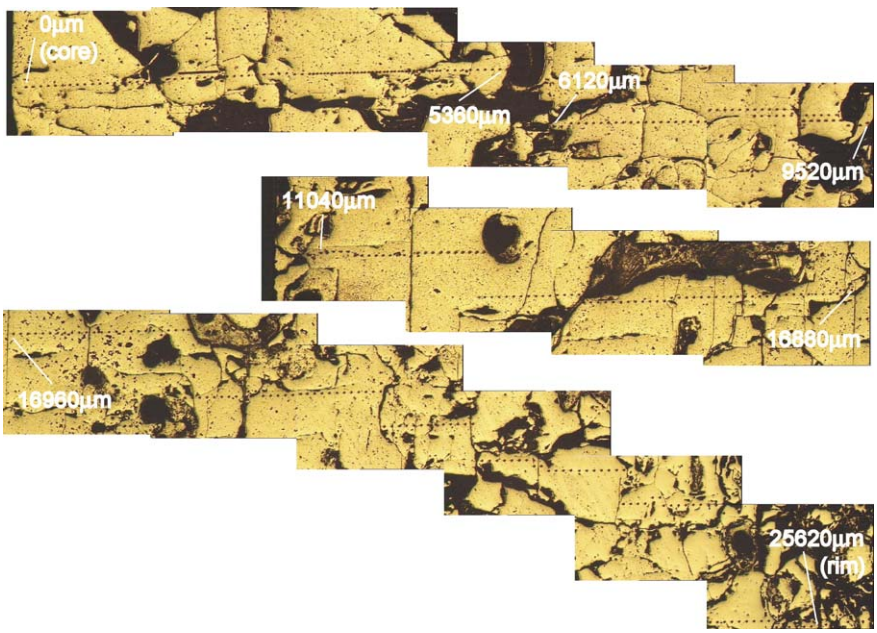

Fig. 3. Ion microprobe traverse from core (0 μm) to rim (25 620 μm) of an intermediate size sanidine megacryst (>5 cm) erupted in the 14.1 ± 1.4 ka dacite lava dome. Two large cracks (5360–6120 μm and 9520–11 040 μm) could not be probed, ion probe spatter pits are evident at 80 μm stepwidth in segments chosen to avoid cracks and holes with the traverse. The area between 3000 and 4800 μm was probed twice due to changes in the calibration of ion microprobe standards.

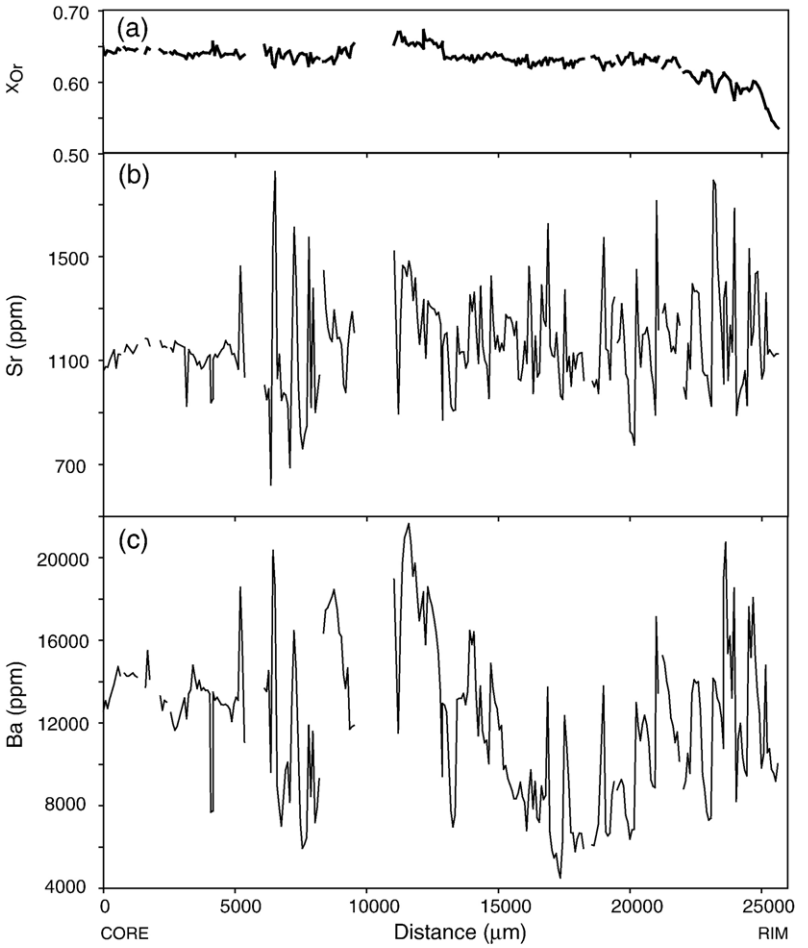

Fig. 4. Geochemical profiles from core to rim of the Taapaca sanidine megacryst. Gaps in the profile are due to cracks in the crystal or analyses of inclusions of plagioclase or oxides, which were filtered from the data discussed here. (a) Orthoclase profile. Variations are small at around 65% orthoclase content, with a drop to more sodic sanidine towards the crystal rim. (b) Sr concentration profile. The crystal core (0–5040 μm) shows little variation around the average of ~1100 ppm, while the remaining profile shows significant short wavelength variations with concentrations ranging from ~600 to ~1800 ppm. Relative errors in Sr concentration are less than 2% (1σ). (c) Ba concentration profile. Again, the crystal core shows relatively little variation around 13 000 ppm, compared to the bulk of the crystals with short wavelength variations ranging between ~4000 and ~22 000 ppm. Relative errors in Ba concentration are less than 2% (1σ).

12 000 to 15 000 ppm for Ba. The remainder of the crystal shows significant variability in trace element concentrations, ranging from 600 to 1800 ppm for Sr and from 4000 to 22 000 ppm for Ba, with wavelength of geochemical variations down to < 160 μm, yielding a very complex crystal growth history.

5. Dating methodology

5.1. Partitioning of Sr and Ba between sanidine and melt

In sanidines, Sr and Ba can substitute for Ca^{2+} as a result of their same charge (Mahood and Stimac, 1990; Blundy and Wood, 1991). Ba may also substitute for K^{+} because of their similarity in ionic radii (Guo and Green, 1989; Icenhower and London, 1996). However, the partitioning of Sr and Ba between sanidine and melt is dominated by magma polymerization (Mysen and Virgo, 1980; Mahood and Stimac, 1990; Ewart and Griffin, 1994; White et al., 2003), and in particular by melt alumina content (Ren, 2004). Sanidine composition appears to play a subordinate role on Sr and Ba partitioning between crystal and melt. The Taapaca sanidine crystal studied here shows very small compositional variations in the proportions of orthoclase (X_{Or} ~0.65, cf. Fig. 4a) and anorthite ($0.004 \leq X_{An} \leq 0.014$). Thus, the uptake of Sr and Ba during crystal growth was almost entirely controlled by

melt composition, and therefore a very similar degree of variability in Sr and Ba content across the crystal would be expected. However, the data in Fig. 5 in contrast show a very good correlation of Sr with Ca, compared to an extremely poor correlation of Ba with Ca. Given the significantly higher diffusivity of Sr compared to Ba within the sanidine structure (cf. Cherniak, 1996, 2002), this suggests that the initial distribution of Sr was modified by intracrystalline diffusion following crystal growth, while the initial distribution of Ba may have remained largely unchanged.

5.2. Bulk crystal diffusion modelling

A simplified version of the model of Zellmer et al. (1999) for intracrystalline diffusion of a trace element step profile towards equilibrium lends itself to the analysis of this crystal (Fig. 6a). The diffusion in each zone of the crystal can be modelled using the solution for diffusion in a layer of half-width w with its edge ($y=w$) at constant interface composition (e.g. Bird et al., 1963, their equation 11.1–31, grey box in Fig. 6a). In the beginning, the amplitudes of the zoning remain constant as diffusion affects only the edges of the zones. Subsequently, zoning amplitudes decrease as chemical equilibration proceeds. Following Zellmer et al. (1999), we define δ as the undiffused fraction of the initial concentration, evaluated at $y=0$. Fig. 6b shows the evolution of δ with time, using a step width $2w=80$ μm as given by the observed wavelengths of geochemical variations, a magmatic temperature of 875 °C (cf. Clavero, 2002), and the Arrhenius relation for the diffusion of Sr in sanidine (Cherniak, 1996). Given that the initial Sr distribution of the sanidine crystal studied here was significantly modified by diffusion (i.e. $\delta<<100\%$), the timescale of crystal residence is estimated to range from a few hundred to a couple of thousand years (cf. Fig. 6b).

5.3. Correlation analysis of geochemical zoning patterns

More detailed insights into the growth history of the crystal may be gained by correlation analysis of geochemical zoning patterns from its core to its rim. Due to the variability in trace element concentration

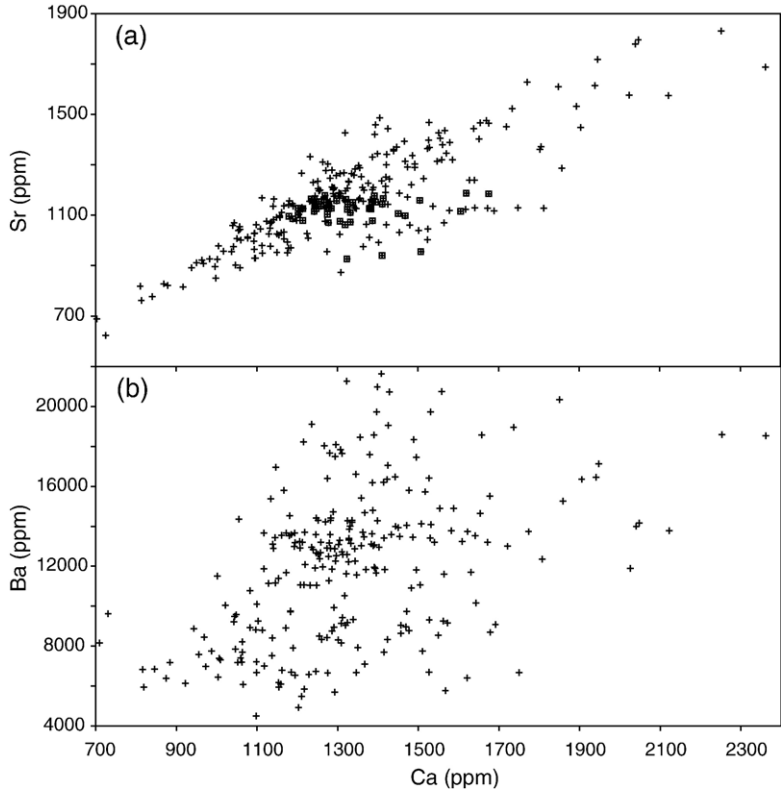

Fig. 5. (a) Sr is relatively well correlated with Ca. Squares are data from the core which shows very limited variation in Sr and little variation in Ca content. (b) Correlation of Ba with Ca for the bulk crystal is very poor.

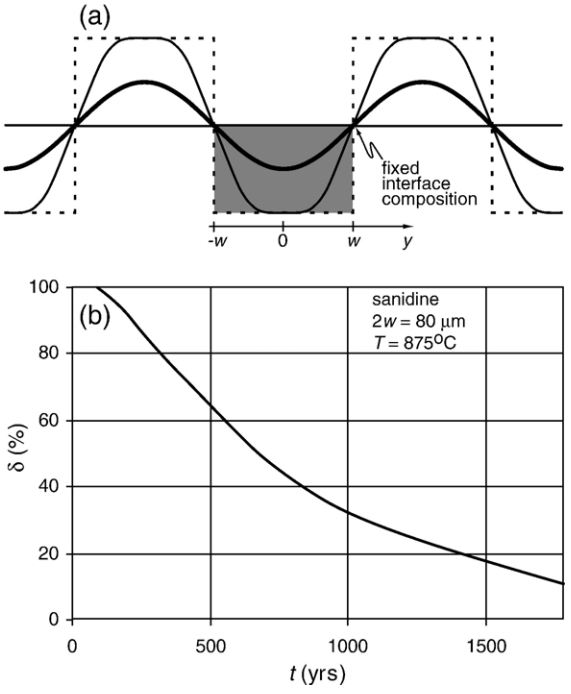

Fig. 6. (a) Model of diffusive destruction of oscillatory zoning. Initially, the crystal has alternating zones of width $2w$ with distinct trace element concentrations. The composition–time–position relationship in a given zone is the same as that for a slab of width $2w$ of given initial composition with the surface composition fixed at the interface (grey box). In the beginning, the amplitudes of the zoning remain constant as diffusion affects only the edges of the zones. Subsequently, zoning amplitudes decrease as chemical equilibration proceeds towards equilibrium. (b) Diffusive destruction of square wave Sr concentration signals with time for the sanidine crystal studied here. δ is the undiffused fraction of the initial square wave concentration profile at $y=0$. See text for discussion.

patterns, it is difficult to assign well-defined growth zones to the traverse, apart from the distinction of a core (0–5040 μm) with low trace element variability and the much larger outer part of the crystal with significantly greater variations (Fig. 4). Overlapping fixed-width segments have therefore been used for correlation analysis, each segment 3120 μm wide, equivalent to 39 data points at 80 μm step width. The variation from core to rim of r^2, the square of the Pearson product moment correlation coefficient (hereafter simply referred to as correlation coefficient) of these fixed-width segments is given in Fig. 7a for the correlations of Sr with Ca and Ba with Ca. Correlation coefficients vary from $r^2=0$ to $r^2=0.95$, but are higher for Sr than for Ba throughout most of the crystal, as would be expected given the significantly better bulk crystal correlation between Sr and Ca (Fig. 5). Note that the core of the crystal is not suitable for correlation analysis due to its low variability of Sr (and to some degree Ca) concentrations. Intracrystalline diffusive equilibration at magmatic temperatures is taken to be responsible for the difference in correlation coefficients of Sr and Ba. This difference is given in Fig. 7b, with the width of the correlation segments indicated by horizontal bars. The effect of different correlation segment widths on this profile is small, e.g. a very similar profile is generated using 25% longer segment widths. It is evident that the correlation difference is generally low where Ba correlation coefficients are relatively high (compare Fig. 7b to Fig. 7a). This is expected if the variability in Sr and Ba content across the crystal was initially very similar (as inferred in Section 5.1), so that subsequent intracrystalline diffusion of Sr would have resulted in a greater improvement of the correlation of Sr with Ca in zones with initially poor correlation. Therefore, zones of high correlation difference are suitable for dating, and it is evident that in these zones the degree of correlation difference decreases approximately linearly from ~0.75 at 9360 μm to ~0.4 at the crystal rim. Thus, while about $\delta=60\%$ of the initial Sr disequilibria are preserved at the crystal rim, only about $\delta=25\%$ are preserved just outbound of its core. Using the above diffusion model for the sanidine crystal studied, the ages of 4 crystal growth zones can therefore be calculated, and they range from ~1300 years near the core to ~550 years near the rim of the crystal (cf. Fig. 7b), yielding an effective crystal growth rate of $\sim 1.2\times10^{-10}$ cm s^{-1}. The ages are in good agreement with results of years to thousands of years obtained by Wöerner et al. (2004) for sanidines from the 32.9±3.6 ka old Taapaca dacite dome, based on Ba diffusion across sharp compositional contrasts revealed by electron microscopy (after Morgan et al., 2004).

6. Discussion

Trace element speedometry is governed by temperature constraints, and the crystal residence times obtained as part of this study are based on the persistence of magmatic temperatures over the calculated timescales. In an alternative scenario, the crystal may have cooled more rapidly and may intermittently have been stored at much lower temperatures for longer periods of time, during which diffusion would have essentially ceased, before being reheated and remobilized due to influx of hot magma from depth. The large sizes of the Taapaca sanidine crystals provide an opportunity to test this scenario by absolute dating of individual growth zones. This has been attempted previously for the 32.9±3.6 ka old Taapaca dacite dome using Ar–Ar geochronology, with a sanidine core

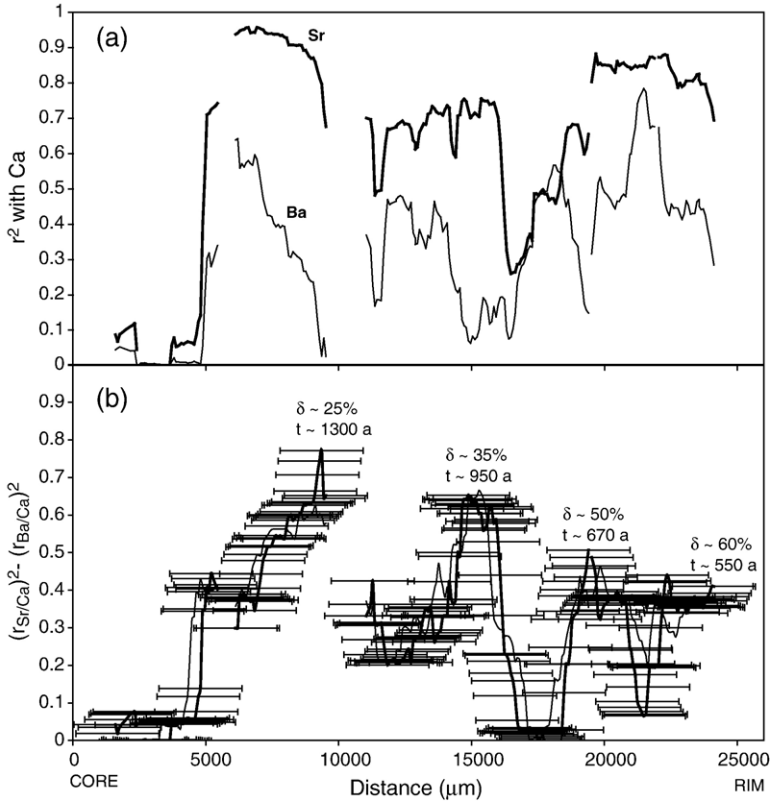

Fig. 7. (a) The variation of the correlation coefficient between Sr and Ca (thick line) and Ba and Ca (thin line) from core to rim of the sanidine crystal, using 3120 μm segments as basis for the correlation (39 data points at 80 μm step width). Correlation of Sr with Ca is better than correlation of Ba with Ca throughout most of the crystal, as expected from Fig. 5. However, there are significant variations in correlation across the crystal. Correlation in the core is extremely poor, due to the low range in Sr and Ba concentrations in this part of the crystal. (b) Subtracting the Ba correlation profile from the Sr correlation profile yields the differential correlation profile (thick line). The width of the correlation segment given by horizontal bars (omitted in a for clarity). The effect of different correlation segment widths on this profile is small, e.g. a very similar profile is generated using a segment width of 3920 μm (thin line). Maxima coincide with zones where Ba correlation is poor, and where correlation of Sr was probably significantly improved due to diffusion at magmatic temperatures. Ages of individual growth zones are calculated using a simple diffusion model (cf. Fig. 6), with 80 μm step width as given by the probe point spacing, at a magmatic temperature of 875 °C. Diffusion coefficients are taken from Cherniak (1996). See text for discussion.

age of 38.6±5.2 ka within error of a rim age of 33.4±3.6 ka (Lohnert, 1999). It is at this point unclear to what degree these ages are affected by Ar diffusion within the crystal. U–Th isochron dating, using separates of mineral inclusions within core and rim of a sanidine megacryst, may also be a useful approach. More precise Ar–Ar dating work (Singer, pers. comm.) and U-series dating of sanidine growth zones (Wörner, pers. comm.) are currently in progress.

Irrespective of the outcome of such studies, a short sanidine megacryst residence time of ~1300 years at magmatic temperatures implies the presence of a rather quickly cooling, ephemeral magma reservoir. If the reservoir takes the form of a sill, a simple conductive cooling model may be employed to estimate its dimension prior to eruption of the dacite. Using a time t of 1300 years and a thermal diffusivity κ of $(4.7 \pm 1.3) \times 10^{-7}$ m^2 s^{-1} (see Appendix), the thickness d of the sill, given by $d=(\kappa t)^{1/2}$, is of the order of 140±20 m, implying a fairly small upper crustal magma reservoir. Greater reservoir dimensions may be possible if convection is operating, although convection within the dacites will be damped due to the high crystallinity of the system (cf. Fig. 1). Small magma reservoirs are consistent with the short wavelength and high amplitude of trace element variabilities within the sanidine megacrysts, as these indicate that the magmatic system is not large enough to buffer open system processes such as assimilation and magma mixing events.

In contrast, the core (0–5040 μm) of the Taapaca sanidine megacrysts studied here exhibits significantly lower trace element variability, indicating that its growth history may have taken place in a very different magmatic environment, presumably in a system with much less

variable melt compositions. It may therefore be speculated that the crystal core grew from a melt that was thermally and compositionally buffered, perhaps from a melt stored in a much larger lower crustal reservoir that was periodically feeding into more ephemeral upper crustal magma chambers, where the compositionally more variable overgrowth would have formed subsequently.

Particularly the younger dacite lava domes of Taapaca volcano contain an abundance of mafic enclaves, which have been interpreted to represent influxing of mafic magma that mingled with and provided heat and volatiles to the more evolved magmas stored in the upper crust, potentially triggering volcanic eruptions. The Taapaca system may in this respect be similar to many other intermediate arc volcanoes, such as Montserrat, where the determination of plagioclase crystal residence times has recently led to very similar ideas of remobilization of small and ephemeral magma reservoirs (cf. Zellmer et al., 2003), and where there is similar evidence for the cyclic pattern of intensive eruptive phases triggered by influx of hot mafic magma, followed by relatively long periods of quiescence (tens of thousands of years), during which there is no evidence of volcanic activity. Clearly, a detailed evolutionary plan of the Taapaca magmatic system cannot be derived on basis of a single megacryst. Nevertheless, this study provides another example that puts constraints on timescales of crystal growth and residence, which, combined with studies of cyclic eruption histories of intermediate arc volcanoes, inform differentiation processes and their rates, and may therefore have significant implications for models of magma transport, storage and crustal differentiation at destructive plate margins.

7. Conclusions

Large sanidine megacrysts are found in many young intermediate arc lavas of the Central Andes. A 14.1±1.4 ka sanidine megacrysts from a dacite lava dome of Taapaca volcano, Northern Chile, displays complex zoning patterns. A relatively homogeneous crystal core is overgrown by zones of high variability in trace element concentrations, with wavelengths of geochemical variations down to <160 μm.

Using trace element correlation patterns and Sr diffusion analysis, individual crystal growth segments can be dated despite the complexities of crystal growth. Ages range from ~1300 years near the crystal core to ~550 years at the crystal rim at a magmatic temperature of 875 °C, yielding an effective growth rate of $\sim 1.2 \times 10^{-10}$ cm s^{-1}.

Short crystal residence times suggest that most of the crystal grew within an ephemeral upper crustal magma reservoir, which is unlikely to have exceeded ~160 m in thickness. Abundant mafic enclaves within the host dacite point to remobilization of the reservoir by hotter, more mafic magma prior to eruption. This is consistent with the observed cyclic behaviour of short and ephemeral episodes of intensive volcanic activity triggered by influx of hot, more mafic magma, followed by longer periods of relative quiescence.

Acknowledgements

We thank Steve Goldstein, Steve Sparks and Gerhard Wörner for useful discussions. Richard Hinton's support at the ion microprobe facility at Edinburgh was much appreciated. This paper benefited from reviews by Frank Tepley and Nobu Shimizu. Ion microprobe analyses were funded by NERC (IMP/159/0400). GFZ acknowledges a Lamont-Doherty Postdoctoral Research Fellowship, a SOEST stipend, and additional financial support by Dave Walker for fieldwork in northern Chile.

Appendix A

The thermal diffusivity κ is related to the thermal conductivity λ through $\kappa = \frac{\lambda}{\rho \cdot C_P}$, where ρ is the density and C_P is the specific heat capacity of a rock. For volcanic rocks with weak radiative component, such as the Taapaca dacites, λ is 1.35±0.15 W m^{-1} K^{-1} at 875 °C (cf. Clauser and Huenges, 1995). Dacites typically have densities of 2500±300 kg m^{-3} (Murase and McBirney, 1973) and specific heat capacities of 1150±250 J kg^{-1} K^{-1} (Bacon, 1977). We therefore obtain a thermal diffusivity of $\kappa = (4.7 \pm 1.3) \times 10^{-7}$ m^2 s^{-1} for the Taapaca dacite lava domes.

References

Allègre, C.J., 1968. ^{230}Th dating of volcanic rocks: a comment. Earth and Planetary Science Letters 5, 209–210.

Allègre, C.J., Condomines, M., 1976. Fine chronology of volcanic processes using ^{238}U–^{230}Th systematics. Earth and Planetary Science Letters 28, 395–406.

Anderson Jr., A.T., 1983. Oscillatory zoning of plagioclase: Nomarski interference contrast microscopy of etched polished sections. American Mineralogist 68, 125–129.

Anderson Jr., A.T., 1984. Probable relations between plagioclase zoning and magma dynamics, Fuego Volcano, Guatemala. American Mineralogist 68, 660–676.

Anderson, A.T., Davis, A.M., Lu, F., 2000. Evolution of Bishop Tuff rhyolite magma based on melt and magnetite inclusions and zoned phenocrysts. Journal of Petrology 41, 449–473.

Bacon, C.R., 1977. High temperature heat content and heat capacity of silicate glasses: Experimental determination and a model for calculation. American Journal of Science 277, 109–135.

Bahat, D., 1979. Anorthoclase megacrysts: physical conditions of formation. Mineralogical Magazine 43, 287–291.

Bird, A.B., Stewart, W.E., Lightfoot, E.N., 1963. Transport Phenomena. Wiley, New York.

Blundy, J.D., Shimizu, N., 1991. Trace element evidence for plagioclase recycling in calc-alkaline magmas. Earth and Planetary Science Letters 102, 178–197.

Blundy, J.D., Wood, B.J., 1991. Crystal-chemical controls on the partitioning of Sr and Ba between plagioclase feldspar, silicate melts, and hydrothermal solutions. Geochimica et Cosmochimica Acta 55, 193–209.

Cashman, K.V., Marsh, B.D., 1988. Crystal size distribution (CSD) in rocks and the kinetics and dynamics of crystallisation. II: Makaopuhi lava lake. Contributions to Mineralogy and Petrology 99, 292–305.

Chapman, N., Powell, R., 1976. Origin of anorthoclase megacrysts in alkali basalts. Contributions to Mineralogy and Petrology 58, 29–35.

Charlier, B.L.A., Zellmer, G.F., 2000. Some remarks on U–Th mineral ages from igneous rocks with prolonged crystallisation histories. Earth and Planetary Science Letters 183, 457–469.

Cherniak, D.J., 1996. Strontium diffusion in sanidine and albite, and general comments on strontium diffusion in alkali feldspars. Geochimica et Cosmochimica Acta 60, 5037–5043.

Cherniak, D.J., 2002. Ba diffusion in feldspar. Geochimica et Cosmochimica Acta 66, 1641–1650.

Christensen, J.N., DePaolo, D.J., 1993. Time scales of large volume silicic magma systems: Sr isotopic systematics of phenocrysts and glass from the Bishop Tuff, Long Valley, California. Contributions to Mineralogy and Petrology 113, 100–114.

Clauser, C., Huenges, E., 1995. Thermal conductivity of rocks and minerals. In: Ahrens, T.J. (Ed.), AGU Reference Shelf 3. Rock physics and phase relations: a handbook of physical constants, pp. 105–126.

Clavero, J., 2002. Evolution of Parinacota Volcano and Taapaca Volcanic Complex, Central Andes of Northern Chile. PhD thesis. University of Bristol, Bristol. 242 pp.

Clavero, J., Sparks, R.S.J., 2005. Geología del Complejo Volcánico Taapaca, Región de Tarapacá, Carta Geológica de Chile, Serie Geología Básica, No. 93, 18p., 1 mapa escala 1:50.000. Servicio Nacional de Geología y Minería, Santiago.

Clavero, J.E., Pérez de Arce, C., Matthews, S., 2004a. High-precision $^{40}Ar/^{39}Ar$ geochronology on sanidine megacrysts from Taapaca Volcanic Complex, Northern Chile. IAVCEI General Assembly, Pucón, Chile.

Clavero, J.E., Sparks, R.S.J., Pringle, M.S., Polanco, E., Gardeweg, M., 2004b. Evolution of Taapaca Volcanic Complex, Central Andes of Northern Chile. Journal of the Geological Society 161, 603–618.

Condomines, M., 1997. Dating recent volcanic rocks through $^{230}Th–^{238}U$ disequilibrium in accessory minerals: example of the Puy de Dome (French Massif Central). Geology 25, 375–378.

Cooper, K.M., Reid, M.R., Murrell, M.T., Clague, D.A., 2001. Crystal and magma residence at Kilauea volcano, Hawaii: $^{230}Th–^{226}Ra$ dating of the 1955 East Rift Eruption. Earth and Planetary Science Letters 184, 703–718.

Costa, F., Chakraborty, S., Dohmen, R., 2003. Diffusion coupling between trace and major elements and a model for calculation of magma residence times using plagioclase. Geochimica et Cosmochimica Acta 67, 2189–2200.

Davidson, J.P., Tepley, F.J., 1997. Recharge in volcanic systems: evidence from isotope profiles of phenocrysts. Science 275, 826–829.

Davidson, J., Tepley, F., Palacz, Z., Meffan-Main, S., 2000. Magma recharge, contamination and residence times revealed by in situ laser ablation isotopic analysis of feldspar in volcanic rocks. Earth and Planetary Science Letters 184, 407–442.

Davies, G.R., Halliday, A.N., 1998. Development of the Long Valley rhyolitic magma system: strontium and neodumium isotope evidence from glasses and individual phenocrysts. Geochimica et Cosmochimica Acta 62, 3561–3574.

Ewart, A., Griffin, W.L., 1994. Application of proton-microprobe data to trace-element partitioning in volcanic rocks. Chemical Geology 117, 251–284.

Gerlach, D.C., Grove, T.L., 1982. Petrology of Medicine Lake Highland volcanics: characterisation of endmembers of magma mixing. Contributions to Mineralogy and Petrology 80, 147–159.

Guo, J., Green, T.H., 1989. Barium partitioning between alkali feldspar and silicate liquid at high temperature and pressure. Contributions to Mineralogy and Petrology 102, 328–335.

Guo, J., Green, T., O'Reilly, S., 1992. Ba partitioning and the origin of anorthoclase megacrysts in basaltic rocks. Mineralogical Magazine 56, 101–107.

Heath, E., Turner, S., Macdonald, R., Hawkesworth, C.J., van Calsteren, P., 1998. Long magma residence times at an island arc volcano (Soufriere, St. Vincent) in the Lesser Antilles: evidence from $^{238}U–^{230}Th$ isochron dating. Earth and Planetary Science Letters 160, 49–63.

Higgins, M.D., 1996a. Crystal size distributions and other quantitative textural measurements in lavas and tuff from Egmont volcano (Mt. Taranaki), New Zealand. Bulletin of Volcanology 58, 194–204.

Higgins, M.D., 1996b. Magma dynamics beneath Kameni volcano, Thera, Greece, as revealed by crystal size and shape measurements. Journal of Volcanology and Geothermal Research 70, 37–48.

Higgins, M.D., 2000. Measurement of crystal size distributions. American Mineralogist 85, 1105–1116.

Hinton, R.W., 1990. Ion microprobe trace-element analysis of silicates: measurement of multi-element glasses. Chemical Geology 83, 11–25.

Humler, E., Whitechurch, H., 1988. Petrology of basalts from the Central Indian Ridge (lat. 25°23′S, long. 70°04′E): estimates of frequencies and fractional volumes of magma injections in a two-layered reservoir. Earth and Planetary Science Letters 88, 169–181.

Icenhower, J., London, D., 1996. Experimental partitioning of Rb, Cs, Sr, and Ba between alkali feldspar and peraluminous melt. American Mineralogist 81, 719–734.

Knesel, K.M., Davidson, J.P., Duffield, W.A., 1999. Evolution of silicic magma through assimilation and subsequent recharge: evidence from Sr isotopes in sanidine phenocrysts, Taylor Creek Rhyolite, NM. Journal of Petrology 40, 773–786.

Kohn, S.C., Henderson, C.M.B., Mason, R.A., 1989. Element zoning trends in olivine phenocrysts from a supposed primary high-magnesian andesite: an electron- and ion-microprobe study. Contributions to Mineralogy and Petrology 103, 242–252.

Lohnert, E., 1999. Chemical variations of a sanidine megacryst and its implications on the pre-eruptive evolution of the Taapaca volcano in

North Chile: Electron microprobe and Sr-isotope studies. Diploma thesis. Georg-August-Universität Göttingen, Göttingen. 116 pp.

Mahood, G.A., Stimac, J.A., 1990. Trace-element partitioning in pantellerites and trachytes. Geochimica et Cosmochimica Acta 54, 2257–2276.

Marsh, B.D., 1988. Crystal size distribution (CSD) in rocks and the kinetics and dynamics of crystallisation. I: theory. Contributions to Mineralogy and Petrology 99, 277–291.

Morgan, D.J., Blake, S., Rogers, N.W., De Vivo, B., Rolandi, G., Macdonald, R., Hawkesworth, C.J., 2004. Timescales of crystal residence and magma chamber volume from modelling of diffusion profiles in phenocrysts: Vesuvius 1944. Earth and Planetary Science Letters 222, 933–946.

Murase, T., McBirney, A., 1973. Properties of some common igneous rocks and their melts at high temperatures. Geological Society of America Bulletin 84, 3563–3599.

Mysen, B.O., Virgo, D., 1980. Trace element partitioning and melt structure: an experimental study at 1 atm pressure. Geochimica et Cosmochimica Acta 44, 1917–1930.

Nakamura, M., 1995. Continuous mixing of crystal mush and replenished magma in the ongoing Unzen eruption. Geology 23, 807–810.

Pearce, T.H., Kolisnik, A.M., 1990. Observations of plagioclase zoning using interference imaging. Earth Science Reviews 29, 9–26.

Pyle, D.M., Ivanovich, M., Sparks, R.S.J., 1988. Magma cumulate mixing identified by U–Th disequilibrium dating. Nature 331, 157–159.

Reid, M.R., Coath, C.D., Harrison, T.M., McKeegan, K.D., 1997. Prolonged residence times for the youngest rhyolites associated with Long Valley Caldera: ^{230}Th–^{238}U ion microprobe dating of young zircons. Earth and Planetary Science Letters 150, 27–39.

Ren, M., 2004. Partitioning of Sr, Ba, Rb, Y, and LREE between alkali feldspar and peraluminous silicic magma. American Mineralogist 89, 1290–1303.

Singer, B.S., Pearce, T.H., Kolisnik, A.M., Myers, J.D., 1993. Plagioclase zoning in mid-Pleistocene lavas from the Seguam volcanic center, central Aleutian arc, Alaska. American Mineralogist 78, 143–157.

Stamatelopoulou-Seymour, K., Vlassopoulos, D., Pearce, T.H., Rice, C., 1990. The record of magma chamber processes in plagioclase phenocrysts at Thera Volcano, Aegean Volcanic Arc, Greece. Contributions to Mineralogy and Petrology 104, 73–84.

Taddeucci, A., Broecker, W.S., Thurber, D.L., 1967. ^{230}Th dating of volcanic rocks. Earth and Planetary Science Letters 3, 338–342.

Turner, S.P., George, R.M.M., Jerram, D.A., Carpenter, N., Hawkesworth, C.J., 2003. Some case studies of plagioclase growth and residence times in island arc lavas from the Lesser Antilles and Tonga, and a model to reconcile apparently disparate age information. Earth and Planetary Science Letters 214, 279–294.

Volpe, A.M., 1992. ^{238}U–^{230}Th–^{226}Ra disequilibrium in young Mt. Shasta andesites and dacites. Journal of Volcanology and Geothermal Research 53, 227–238.

Volpe, A.M., Hammond, P.E., 1991. ^{238}U–^{230}Th–^{226}Ra disequilibria in young Mount St. Helens rocks: time constraint for magma formation and crystallisation. Earth and Planetary Science Letters 107, 475–486.

White, J.C., Holt, G.S., Parker, D.F., Ren, M., 2003. Trace element partitioning between alkali feldspar and peralkalic quartz trachyte to rhyolite magma, part I: systematics of trace element partitioning. American Mineralogist 88, 316–329.

Woerner, G., Wegner, W., Kiebala, A., Singer, B.S., Heumann, A., Kronz, A., Hora, J., 2004. Evolution of Taapaca volcano, N. Chile, evidence from major and trace element, Sr-, Nd-, Pb-, and U-series isotopes, age dating and chemical zoning in sanidine megacrysts. IAVCEI General Assembly, Volcanism and its impact on society, Pucon, Chile.

Zellmer, G.F., Blake, S., Vance, D., Hawkesworth, C., Turner, S., 1999. Plagioclase residence times at two island arc volcanoes (Kameni islands, Santorini, and Soufriere, St. Vincent) determined by Sr diffusion systematics. Contributions to Mineralogy and Petrology 136, 345–357.

Zellmer, G.F., Turner, S.P., Hawkesworth, C.J., 2000. Timescales of destructive plate margin magmatism: new insights from Santorini, Aegean volcanic arc. Earth and Planetary Science Letters 174, 265–282.

Zellmer, G.F., Sparks, R.S.J., Hawkesworth, C.J., Wiedenbeck, M., 2003. Magma emplacement and remobilisation timescales beneath Montserrat: insights from Sr and Ba zonation in plagioclase phenocrysts. Journal of Petrology 44, 1413–1431.

Zinner, E., Crozaz, G., 1986. A method for the quantitative measurement of rare earth elements in the ion microprobe. International Journal of Mass Spectrometry and Ion Processes 69, 17–38.